energy&fuels

Biofuels and Biomass

Application potassium ion impregnated titanium dioxide as nanocatalyst for transesterification of linseed oil.

Indu Ambat, Varsha Srivastava, Esa Haapaniemi, and Mika Sillanpää

Energy Fuels, **Just Accepted Manuscript** • DOI: 10.1021/acs.energyfuels.8b03310 • Publication Date (Web): 27 Oct 2018

ACS Publications

is published by the American Chemical Society. 1155 Sixteenth Street N.W., Washington, DC 20036

Application potassium ion impregnated titanium dioxide as nanocatalyst for transesterification of linseed oil

Indu Ambat[a]*, Varsha Srivastava[a], Esa Haapaniemi[b], Mika Sillanpää[a]

[a] Department of Green Chemistry, School of Engineering Science, Lappeenranta University of Technology, Sammonkatu 12, FI-50130 Mikkeli, Finland

[b] Department of Organic Chemistry, University of Jyväskylä, Finland

*Corresponding Author (email: indu.ambat@outlook.com)

Abstract

The current work comprises the investigation of biodiesel production from linseed oil using TiO_2 and potassium L-tartrate monobasic ($C_4H_5KO_6$) modified TiO_2 nanocatalyst. The different molar ratio of $C_4H_5KO_6$ was selected for TiO_2 modification. The nanocatalyst TiO_2-$0.5C_4H_5KO_6$ (1:0.5 molar ratio) showed the best conversion rate for biodiesel. Nanocatalyst was characterized by FTIR, XRD, TEM, BET, XPS and Hammett indicators benzene carboxylic acid titration method for basicity measurement. The characterization of biodiesel was performed with GC-MS, ^1H and ^{13}C NMR. Furthermore, the optimum reaction parameters for transesterification reaction was analyzed and yield was determined by GC-MS and ^1H NMR. The maximum yield of 98.5 % was obtained at 6 wt% catalyst amount,

1:6 methanol to oil ratio at 60 °C for 3 hours. The properties of biodiesel obtained from linseed oil were determined using EN 14214/ ASTM D6751 method. The reusability of catalyst was tested up to five cycles and it showed promising results.

Key words: Biodiesel, linseed oil, transesterification, TiO_2- $C_4H_5KO_6$ nanocatalyst

1. Introduction

The energy crisis is one of the major issue confronted by the whole world due to the dependency on conventional energy reserves[1,2]. In recent days, with an increase in population results in the expeditious utilization of fossil fuels which leads to two major issues, direct environmental pollution and global warming[2-4]. Biodiesel is fatty acid methyl esters (FAME), has been suggested as suitable alternative fuel which is produced by the transesterification of fats/ oils using alcohol mainly methanol or ethanol with a suitable catalyst[5-8]. FAME can act as a renewable source of energy due to its features such as biodegradability and eco-friendly nature[9].

Generally, vegetable oils, algal oils and animal fat/oils are used as feedstock for biodiesel production[10-12]. The feedstock used for the biodiesel production is preferred to be less expensive as well as does not compete with food production[13,14]. Hence linseed oil was used as feedstock for biodiesel production. Furthermore, the oil content of linseed oil is almost

similar to edible oil such as rapeseed oil and higher than that of soybean and sunflower oil. Moreover, the content of linolenic acid ($C_{18:3}$) was higher compared to other oils[13]. Kumar et al.,[15] reported 88-96 % conversion efficiency of linseed oil with alkali transesterification. Gargari and Sadrameli[16] observed FAMEs yield up to 98.08% in presence of di-ethyl ether as a co-solvent and calcium oxide as a heterogeneous based catalyst in a fixed bed reactor.

The transesterification reaction is commonly conducted using homogeneous catalyst, heterogeneous catalyst, biocatalyst[8,9,13,17]. Currently, heterogeneous nanocatalysts attained greater attraction in the field of biodiesel production due to its features such as increased stability, activity, and selectivity[5,17,18]. Based on previous research reports recommends that potassium doped metal oxides provides promising results in biodiesel production, out of those studies potassium doped on titanium dioxide (TiO_2) using potassium bitartrate as precursor resulted in good biodiesel yield with both edible and non-edible oils[3,8, 19-22]. Additionally, TiO_2 alone serves as a catalyst for transesterification and also acts as good support in heterogeneous catalysis due to its high chemical stability, thermal constancy and commercial availability[7,23]. Therefore potassium impregnated on titania using potassium bitartrate as precursor used for biodiesel production from linseed oil.

In the present study is targeted on the production of biodiesel from linseed oil using heterogeneous nanocatalyst. The purpose of our work is to investigate the effect of heterogeneous nanocatalysis on linseed oil, which has not been explored yet. Hence potassium impregnated TiO_2 as a nanocatalyst was synthesized. The loading effect of $C_4H_5KO_6$ on catalytic activity was also investigated. The TiO_2 -0.5 $C_4H_5KO_6$ nanocatalyst showed the significant conversion of linseed oil to biodiesel. The characterization of

synthesized nanocatalyst was done using Fourier transform infrared spectroscopy (FTIR), Scanning electron microscopy (SEM), X-ray diffraction (XRD), X-ray photoelectron spectroscopy (XPS), Transmission electron microscopy (TEM), Atomic-force microscopy (AFM) and Brunauer-Emmett-Teller (BET). Further, the nanocatalyst has been used for transesterification reaction, where the production conditions such as temperature molar ratio of oil and methanol, catalyst amount and time were optimized. The biodiesel was analyzed by gas chromatography with a mass spectrometry (GC-MS), ^{1}H and ^{13}C nuclear magnetic resonance (NMR).

2. Materials and methods

2.1 Material

Linseed oil (acid value =0.606 mg KOH/g, average molecular weight=887.9354), titanium oxide nanopowder (TiO_2), Potassium bitartrate ($C_4H_5KO_6$), methanol were purchased from Sigma-Aldrich. All the chemicals used were of analytical grade

2.2 Synthesis and screening of catalyst

The titanium dioxide modified by $C_4H_5KO_6$ was synthesized by the impregnation method. In this method, catalysts were prepared by mixing $TiO_2/C_4H_5KO_6$ in different molar ratios of 1:0.25, 1:0.5, 1:0.75 and 1:1. The solutions were stirred continuously for 5h and subsequently dried at 90°C. Finally, dried samples were calcined at 500°C in the muffle furnace (Naberthermb180). The TiO_2, a series of synthesized catalysts by mixing of $TiO_2/C_4H_5KO_6$ in various molar ratios were screened for fatty acid methyl ester (FAME) production. Furthermore, synthesis of series of the catalyst by doping of various concentration of potassium ion to titania helps to investigate the capability of different catalyst in the transesterification of linseed oil as well as it provides the effect of $C_4H_5KO_6$ loading on the catalytic activity of titanium oxide.

2.3 Characterization of catalyst

The FTIR of catalysts were recorded using Vertex 70 Bruker in the range of 400- 4000 cm^{-1}. TEM images of the samples were obtained using HT7700 (Hitachi). The nanocatalyst was dispersed in ethanol with help of sonication, in order to obtain dispersed particles on the suspension. Later a drop of suspension was added to the carbon-coated copper grid. SEM images of catalysts were recorded by spreading sample on colloidal graphite with 5 kV accelerating voltage (SEM, Hitachi SU3500). XRD patterns were obtained with PANalytical – Empyrean X-ray diffractometer over a 2θ range of 10-120º with an X-ray source Co-Kα of 0.178 nm at 40 mA and 40 kV. The surface area of catalyst was determined using BET (BET,

Micromeritics Tristar II plus). The catalyst samples were degassed at 80°C for overnight to remove the moisture from the samples.

AFM (Park Systems NX10) images of nanocatalyst were also collected for better illustration of nanocatalyst. The surface composition and the binding energies of elements in nanocatalyst were examined by ESCALAB 250 model XPS with an Al-K X-ray source of 1486.6 eV. The basicity test of catalyst was performed with help of Hammett indicator benzene carboxylic acid titration method. Hammett indicator–benzene carboxylic acid (0.02 mol L^{-1} anhydrous methanol solution) titration method was performed to determine basic strength of synthesized catalyst using Hammett indicators such as neutral red (H_6.8), bromothymol blue (H_7.2), phenolphthalein (H_9.8), 2, 4 - dinitroaniline (H_15)[24,25] .

2.4 Biodiesel production

Linseed oil was used as feedstock for biodiesel production. The screening of different catalyst was done by performing the reaction by mixing oil to methanol in 1:6 molar ratio and with 6 wt % of each catalyst. All the reactions were carried out in a 250ml three neck round bottom flask with mechanical stirrer and reflux condenser at 60°C for 3h. After the reaction, the samples were centrifuged, resulted in three separate phases such as catalyst at the bottom, methyl ester at top and glycerol at the middle. The catalyst was isolated, excess methanol was removed by the evaporator and the obtained biodiesel was analyzed by GC-MS (Agilent-GC6890N, MS 5975) with an Agilent DB-wax FAME analysis GC column

dimensions 30 m, 0.25 mm, 0.25 µm. The inlet temperature was 250°C and oven temperature was programmed at 50°C for 1 min and it raises at the rate of 25°C/min to 200°C and 3°C /min to 230°C and then it was held for 23 min. The concentration and presence of ester carbonyl groups of fatty acid methyl esters were determined by ^{1}H NMR and ^{13}C NMR at 400 MHz with $CDCl_3$ as solvent, respectively. The percentage of linseed oil conversion to fatty acid methyl esters (C %) was determined by the equation given below[13].

$$C(\%) = \frac{2 \times Intergration\ value\ of\ protons\ of\ methyl\ ester}{3 \times Intergraton\ value\ of\ methyl\ protons} \times 100 \quad (Eq.\ 2)$$

3. Result and discussion

3.1. Screening and selection of nanocatalyst for transesterification of linseed oil

The selection of nanocatalyst for the biodiesel production from linseed oil was obtained by screening of the catalytic activity of different catalyst such as TiO_2, $TiO_2/C_4H_5KO_6$ (1:0.25, 1:0.5, 1:0.75 and 1:1 molar ratios) at 60°C with 6 wt % of each catalyst and 1:6 oil to methanol molar ratio for 3h. The catalyst composition, surface area, total basicity of synthesized catalyst and catalytic performance of each catalyst was indicated in Table1. Basic nature and total basicity of synthesized catalyst was determined by Hammett indicator-benzene carboxylic acid titration method [8, 24-26]. The TiO_2 showed no reaction and it is probably due to lower basic strength. Later the basicity of catalyst rises with the loading

amount of $C_4H_5KO_6$ that increases the activity of the catalyst. Further increase in the $C_4H_5KO_6$ amount after optimum value, reduces the catalytic activity possibly due to a decrease in both surface area and basicity. The $TiO_2/C_4H_5KO_6$ with 1:0.5 ratio showing the significant conversion of biodiesel from linseed oil due to the optimum loading of $C_4H_5KO_6$. Therefore, TiO_2-0.5$C_4H_5KO_6$ was selected for the optimization of reaction parameters for higher production of biodiesel.

Table 1.

The efficiency of various catalyst for transesterification of linseed oil

No.	Catalyst	Molar ratio	Total basicity (mmol g^{-1})	BET surface area (m^2g^{-1})	FAME conversion (%)
1	TiO_2	-	0.1	37.58	No reaction
2	$TiO_2/C_4H_5KO_6$	1:0.25	0.3	25.43	‹5
3	$TiO_2/C_4H_5KO_6$	1:0.5	1.80	16.25	98.54
4	$TiO_2/C_4H_5KO_6$	1:0.75	1.56	10.65	80.10
5	$TiO_2/C_4H_5KO_6$	1:1	0.89	7.37	50.88

3.2. Characterization of catalyst

The FTIR peaks of unmodified TiO_2 and TiO_2-0.5$C_4H_5KO_6$ were shown in Figure1. In the FTIR spectrum of TiO_2-0.5 $C_4H_5KO_6$ shows new peaks at 895.82 cm^{-1}, 1368.324 cm^{-1} and

1458.00 cm^{-1}. New peaks could be due to the integration of potassium ions into the TiO_2 structure. However, it also indicates broadband in range of 2900 cm^{-1} to 3300 cm^{-1} due to stretching vibrations of Ti-O-K bond[3,19].

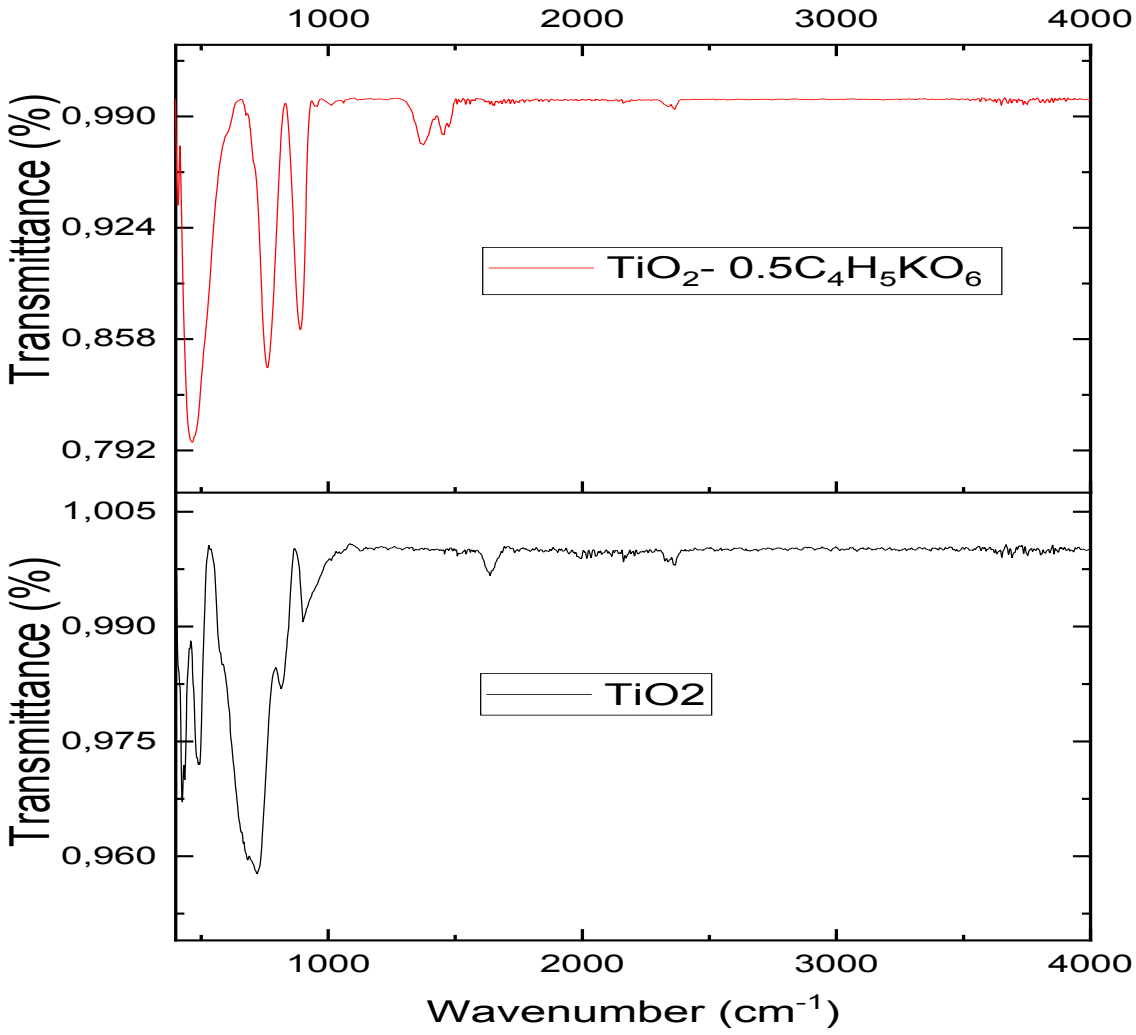

Figure 1. FTIR spectra of TiO_2 (unmodified) and TiO_2-$C_4H_5KO_6$ (1:0.5molar ratio)

Figure 2 shows the XRD pattern of both unmodified TiO_2 and TiO_2-0.5$C_4H_5KO_6$. X-ray diffraction (XRD) analysis of unmodified TiO_2 depicts a good match to standard reference code ICSD: 154607, ICDD: 98-015-4607. XRD pattern of Potassium Titanium Oxide obtained as result of modification of TiO_2 with 0.5 molar $C_4H_5KO_6$ provides a consistent harmony to reference standard code ICSD:73465, ICDD:98-007-3465. The crystallographic parameters of synthesized catalysts are shown in Table 2.

Table 2.

The crystallographic parameters of unmodified TiO_2 and TiO_2-0.5$C_4H_5KO_6$.

Catalyst	**Crystal structure**	**a**	**b**	**c**	**α**	**β**	**γ**
		(nm)	(nm)	(nm)			
TiO_2	Tetragonal	0.379	0.379	0.941	90	90	90
TiO_2-0.5$C_4H_5KO_6$	Tetragonal	1.02	1.02	0.296	90	90	90

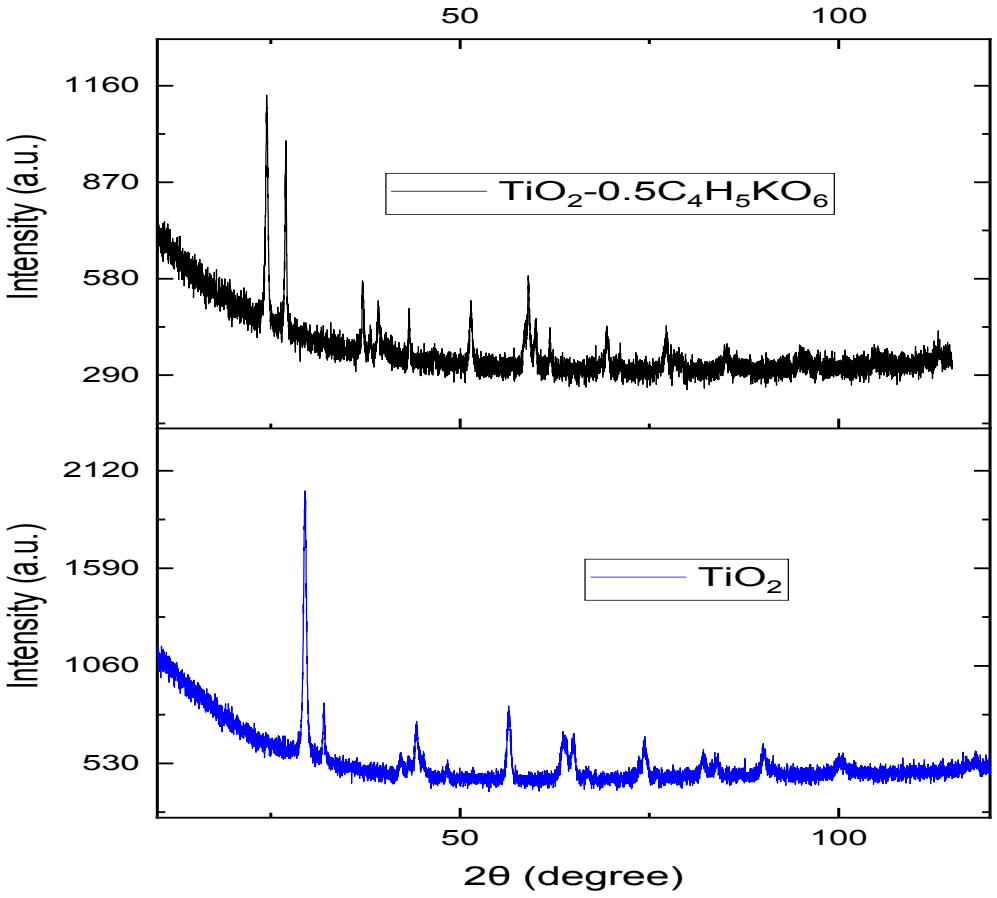

Figure 2. XRD pattern of TiO_2 (unmodified) and TiO_2-$C_4H_5KO_6$ (1:0.5molar ratio)

Surface morphology of catalyst was analyzed by SEM. Figure 3a and 3b show the SEM images of TiO_2 (unmodified) and TiO_2-$C_4H_5KO_6$ (1:0.5molar ratio) with 5kV magnification respectively. By comparing two images, it was observed that there was a significant difference in the structure of TiO_2-$C_4H_5KO_6$ (1:0.5molar ratio) due to the doping of potassium. The unmodified TiO_2 catalyst looks fluffier and comparatively uniform particles with some aggregates. It is very clear from SEM image of TiO_2- $0.5C_4H_5KO_6$ that flat surface of different shapes was dispersed in the catalytic material indicates a different

morphology of particles due to impregnation of potassium particles on the surface of TiO_2 (Figure 3b).

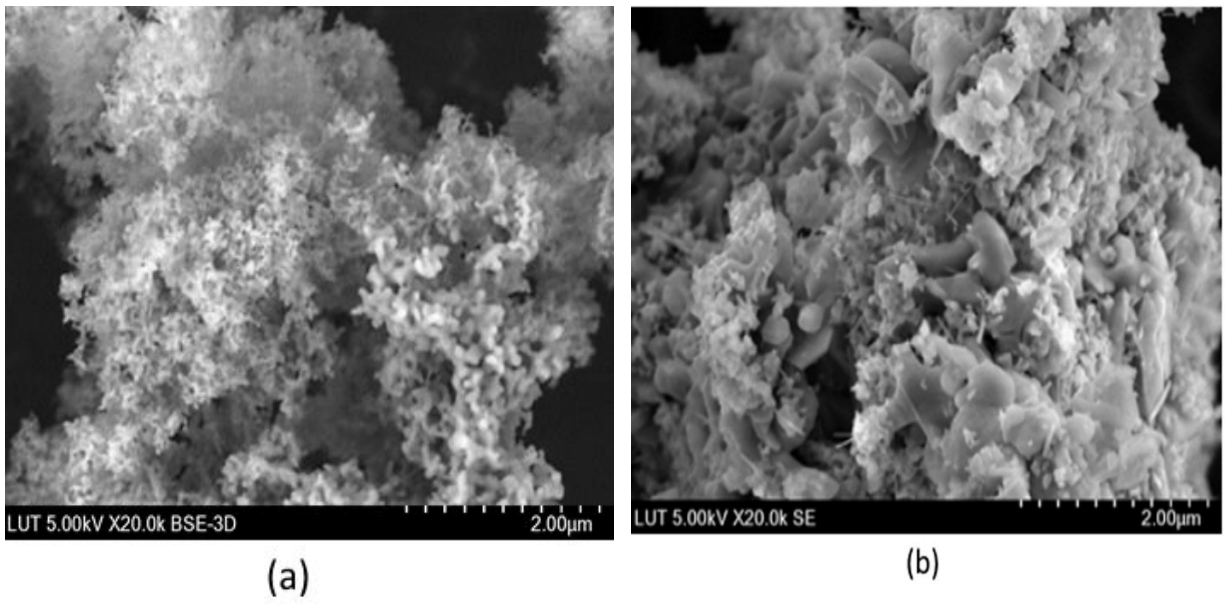

Figure 3. SEM images of (a) unmodified –TiO_2 (b) TiO_2-$C_4H_5KO_6$ (1:0.5molar ratio)

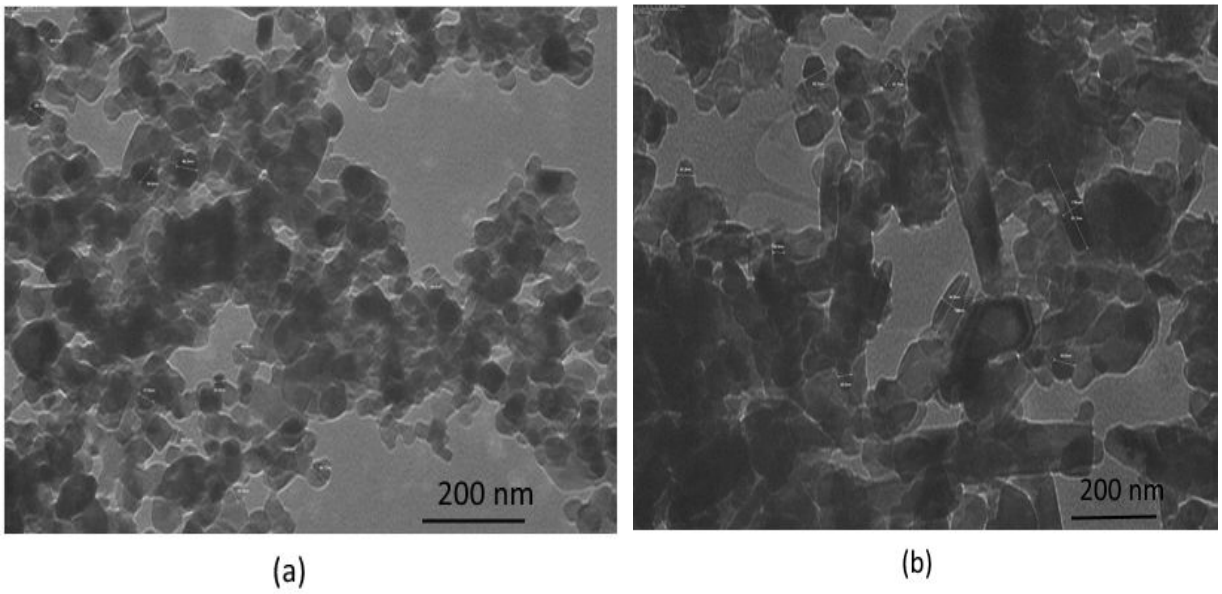

Figure 4. TEM image of (a) unmodified –TiO_2 and (b) TiO_2-$C_4H_5KO_6$ (1:0.5molar ratio)

The TEM image of TiO_2 (unmodified) and TiO_2-$C_4H_5KO_6$ (1:0.5molar ratio) were depicted in Figure 4a and 4b respectively. The TiO_2 (unmodified) catalyst has a particle size of 23- 46.7nm whereas TiO_2-$C_4H_5KO_6$ (1:0.5molar ratio) modified catalyst has a particle size of 26-179nm. The size of the particle in the catalyst was confirmed with help of TEM images. Moreover, TEM image of TiO_2 (unmodified) also represents a well distributed large quantity of uniform particle with agglomerates, while TEM studies of TiO_2-$0.5C_4H_5KO_6$ show long flat structure in addition to uniform particles with aggregates. SEM results also match with TEM images.

The AFM image of TiO_2 and TiO_2-$C_4H_5KO_6$ were portrayed Figure 5 (a, b) with scan rate and amplitude of 0.26Hz and 15.04E3 nm respectively. AFM image also agrees with the

integration of potassium ions into titanium dioxide nanocatalyst. All the dimensions were shown in nanoscale. Particle dimensions measured with AFM images well agreed with TEM analysis and supported potassium loading. All the catalyst characterization confirms the impregnation of potassium ion to titania.

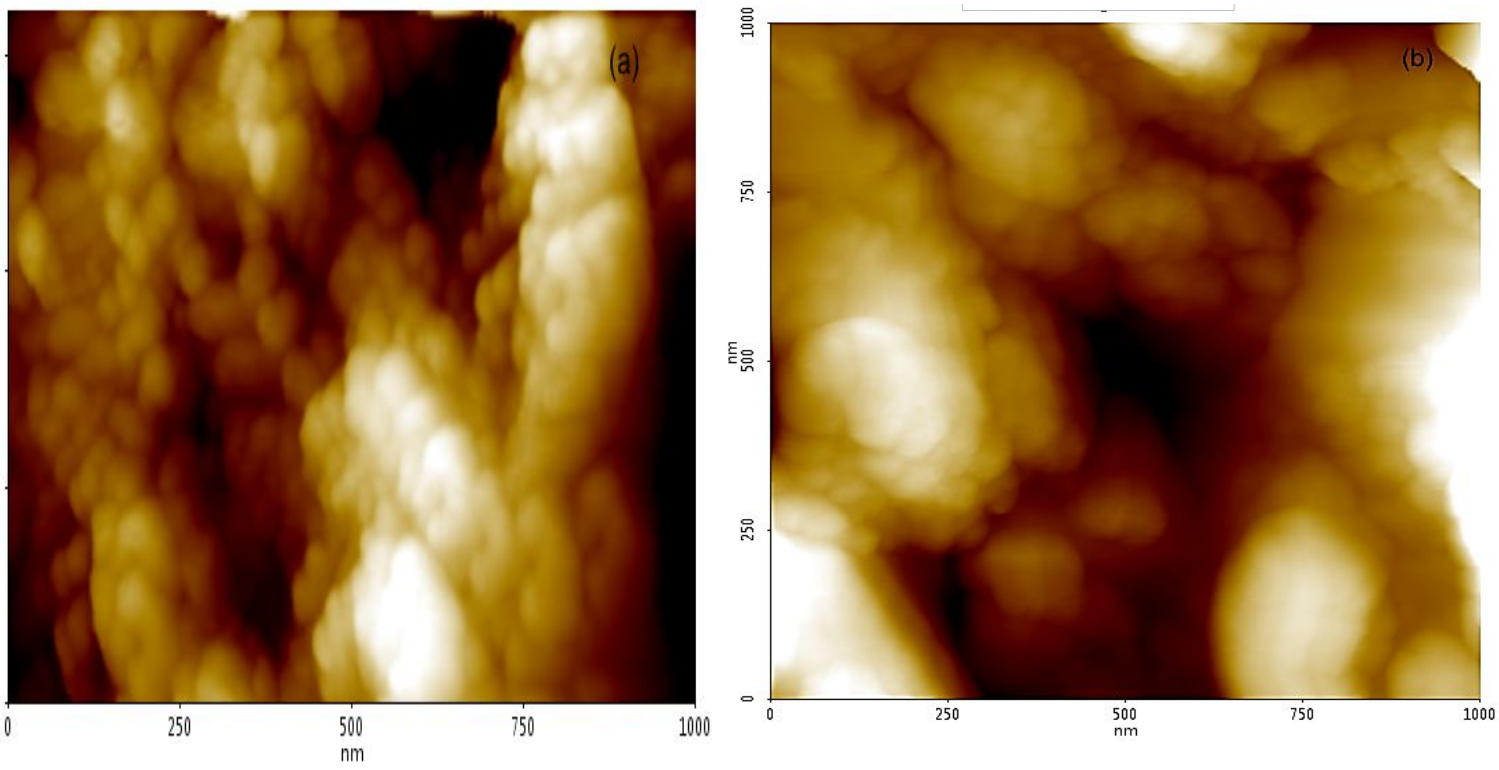

Figure 5. Depicts AFM image of (a) unmodified –TiO_2 (b) TiO_2-$C_4H_5KO_6$ (1:0.5molar ratio)

The surface area, pore volume and pore size were determined by BET analysis. The surface area analysis of unmodified –TiO_2 and TiO_2 – 0.5 $C_4H_5KO_6$ using BET is shown in Table 3. The decrease in porosity of TiO_2 modified with $C_4H_5KO_6$ catalyst was due to the insertion of potassium ions[25]. Even though there is a decrease in porosity and surface area, but there is an increase in catalytic activity for transesterification which is depicted in Table 1. It may be due the action of the strength of basic sites in the catalyst[25]. The N_2 adsorption-desorption isotherm for TiO_2 and TiO_2 modified with $C_4H_5KO_6$ from BET analysis is given in Figure 6. The hysteretic loop isotherm indicates the presence of mesoporous materials.

Table 3.

The results of Brunauer-Emmett-Teller surface area analysis

	Parameters	Unmodified TiO_2	TiO_2 - $C_4H_5KO_6$ (1:0.5 molar ratio)
Surface area	BET surface area (m^2/g)	37,58	16,25
	BJH adsorption cumulative surface area of pores (m^2/g)	34,32	12,49
	BJH desorption cumulative surface area of pores (m^2/g)	34,41	12,75

Pore volume	Single point adsorption total pore volume of pores (cm^3/g)	0,06	0,03
	BJH adsorption cumulative volume of pores (cm^3/g)	0,10	0,09
	BJH desorption cumulative volume of pores (cm^3/g)	0,11	0,09
Pore size	Adsorption average pore width (A°)	64,31	72,43
	BJH adsorption average pore diameter (A°)	122,41	296,76
	BJH desorption average pore diameter (A°)	129,24	291,11

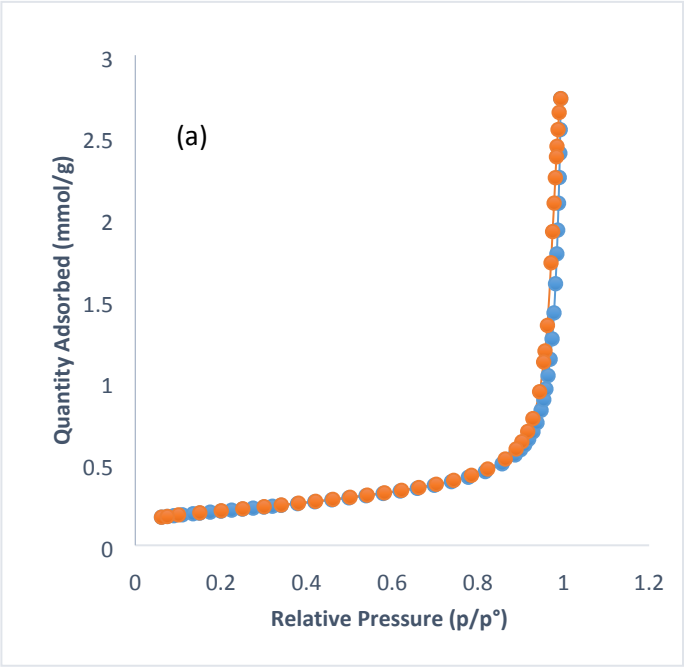

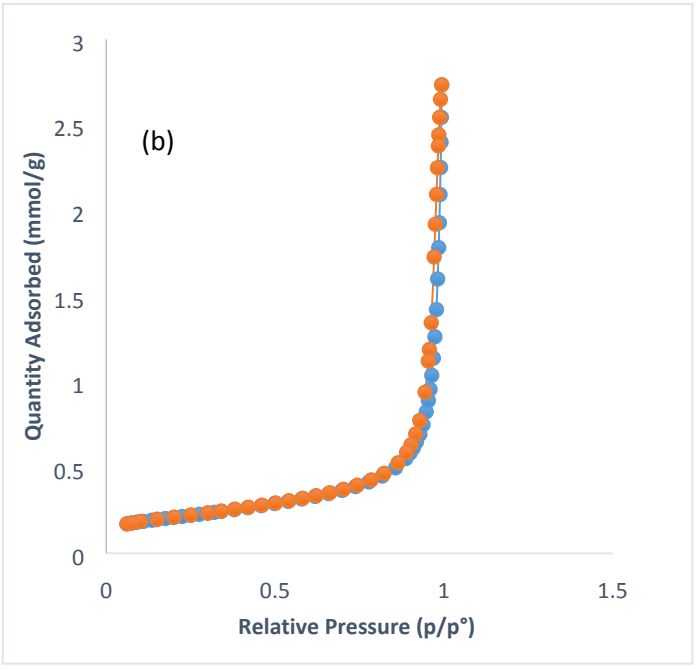

Figure 6. N_2 adsorption-desorption of (a) unmodified $-TiO_2$ (b) TiO_2-$C_4H_5KO_6$ (1:0.5molar ratio)

XPS was applied to examine the surface properties and binding energies (BE) of elements in unmodified $-TiO_2$ (b) TiO_2-$C_4H_5KO_6$ (1:0.5molar ratio). The chemical environment of Ti, O, K were simulated by Gaussian curve-fitting of the Ti 2p, K 2p and O 1s spectra of unmodified $-TiO_2$ and TiO_2-$0.5C_4H_5KO_6$. Figure 7 (a) and (b) depicts XPS fitted spectra of unmodified $-TiO_2$ and TiO_2-$0.5C_4H_5KO_6$ nanocatalyst. Both in unmodified $-TiO_2$ and TiO_2-$0.5C_4H_5KO_6$ depict Ti 2p signals with two peaks at binding energies of 463.66 and 457.96 eV assigned to Ti $2p_{1/2}$ and $2p_{3/2}$, respectively. The BE gap between these two core level orbital suggesting that chemical valance state of Ti in synthesized nanocatalyst is +4. The O 1s spectra of unmodified $-TiO_2$ and TiO_2-$0.5C_4H_5KO_6$ shows binding energy at 530.1 eV, which corresponds to O^{2+} forming oxide with metals [27]. Figure 7b. represents K 2p with binding energies at 292.37 eV and 294.97 eV which is assigned to $2p_{3/2}$ and $2p_{1/2}$ in the K–O group of TiO_2-$0.5C_4H_5KO_6$ [28].

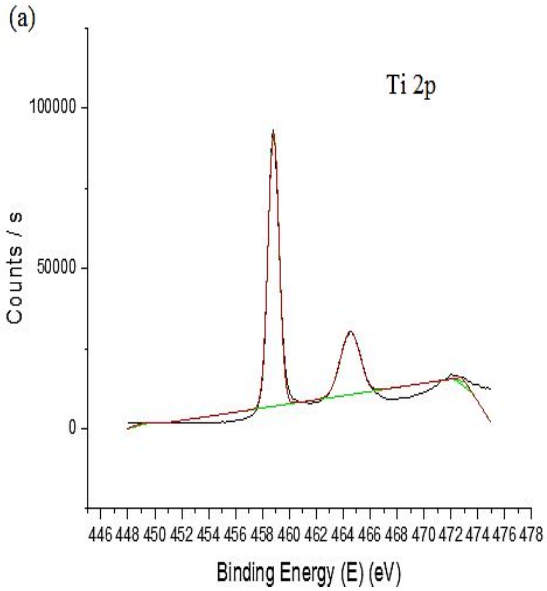
(a)
Ti 2p
Counts / s
Binding Energy (E) (eV)

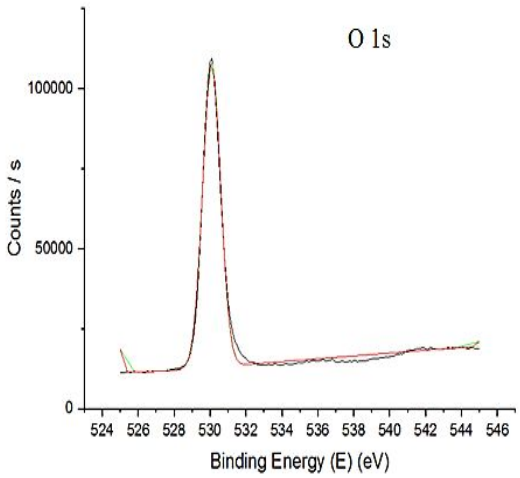
O 1s
Counts / s
Binding Energy (E) (eV)

244

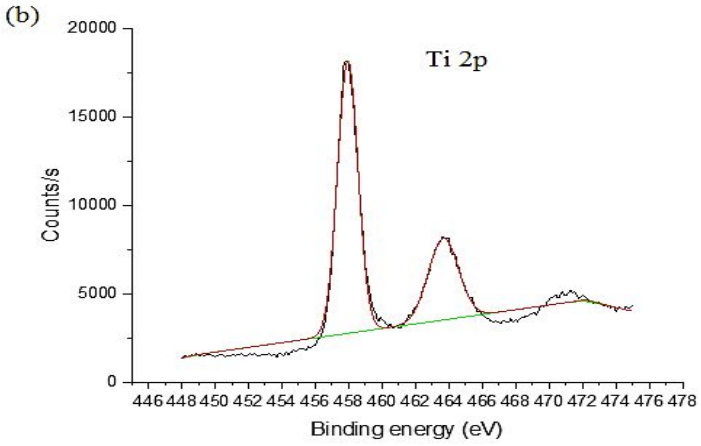
(b)
Ti 2p
Counts/s
Binding energy (eV)

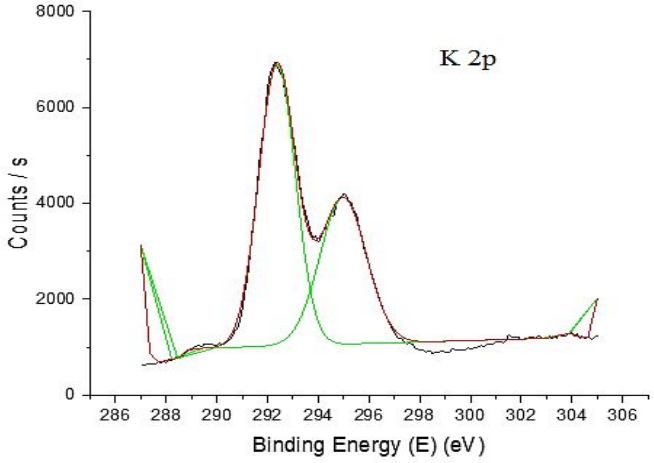
K 2p
Counts / s
Binding Energy (E) (eV)

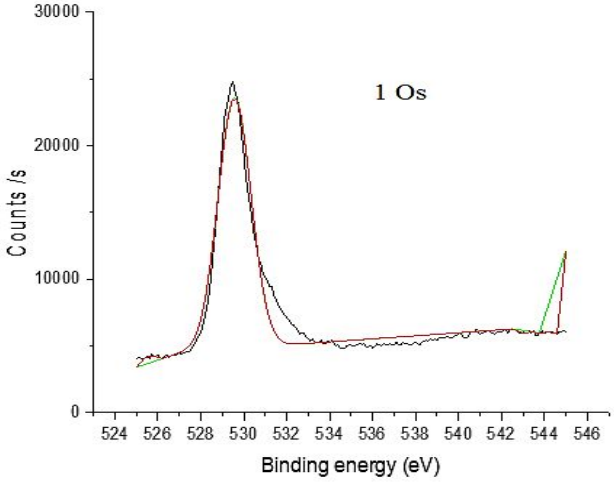
1 Os
Counts /s
Binding energy (eV)

Figure 7. XPS spectra of (a) unmodified –TiO_2 (b) TiO_2-$C_4H_5KO_6$ (1:0.5molar ratio)

3.3. Characterization of biodiesel

The fatty acid methyl esters made from the linseed oil was characterized by GC-MS, ^1H NMR and ^{13}C NMR. The quality of the produced biodiesel was tested using the EN 14214/ ASTM D6751 method

The chemical composition of biodiesel was demonstrated with the help of GC-MS chromatogram and National Institute of Standards and Technology (NIST) 2014 MS library. The component of biodiesel obtained after transesterification of linseed oil with TiO_2 – 0.5 $C_4H_5KO_6$ was recognized with the help of a library match and represented in Table 4.

Table 4.

The composition of biodiesel attained after transesterification with TiO_2- 0.5 $C_4H_5KO_6$.

Peak	**FAME**		**Compound name & mass spectrum**
	Retention time (min)	Library match (%)	

1	8.38	91.2	Hexadecanoic acid, methyl ester 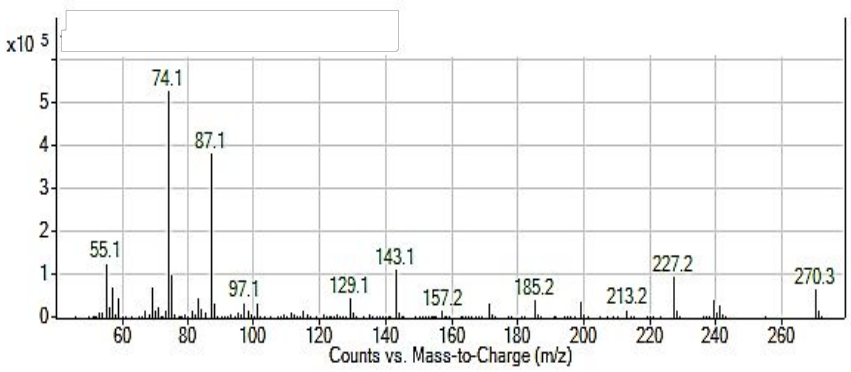
2	9.89	93.6	Methyl stearate 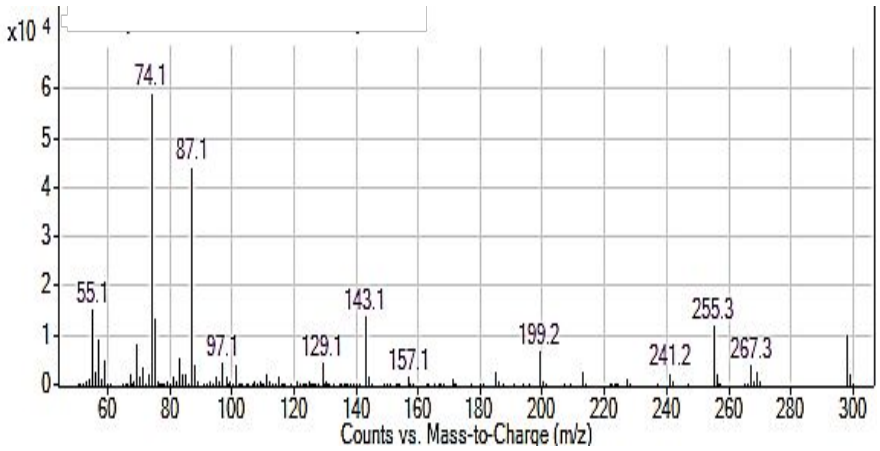
3	10.09	94	9-Octadecenoic acid, methyl ester 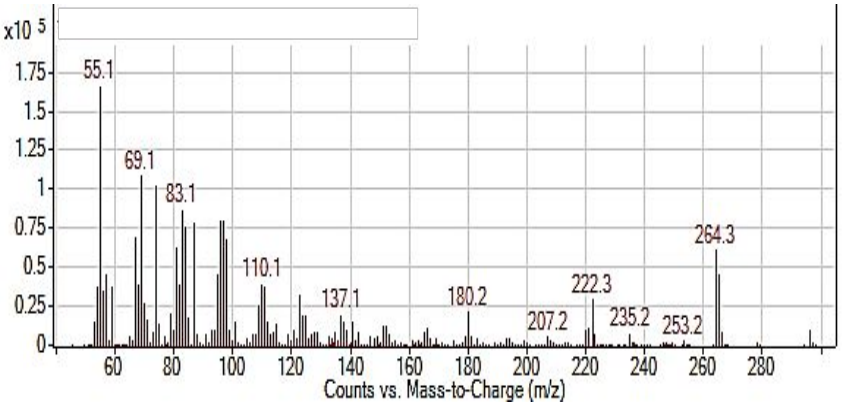
6	10.48	94.3	9, 12- Octadecenoic acid (Z,Z)-, methyl ester

			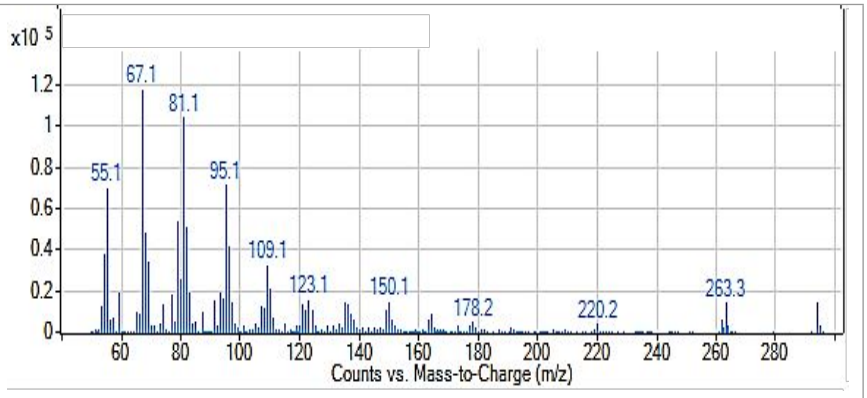
7	11.19	92.9	9,12,15 Octadecatrienoic acid, methyl ester 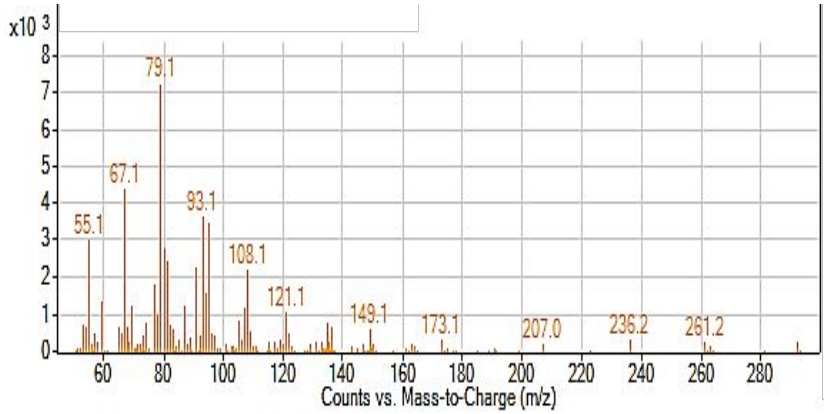

The analysis of fatty acid methyl esters of linseed oil was conducted by ^{1}H and ^{13}C NMR spectroscopy. The biodiesel yield was calculated using equation 2, which was already mentioned above. With the help of ^{1}H NMR, FAME conversion percentage of sample obtained after transesterification with TiO_2- $0.5C_4H_5KO_6$ was found to be 98.5 %. Figure 8a and 8b illustrate the ^{1}H NMR and ^{13}C spectrum of fatty acid methyl esters sample obtained with help of TiO_2- $0.5C_4H_5KO_6$ catalyst respectively. It helps to characterize FAME and can be used to conform the existence of methyl esters in the biodiesel. Moreover, the proposed

catalyst resulted in better conversion of linseed oil to biodiesel in comparison with previously reported studies using alkali as well as CaO as solid catalyst [15,16].

In ^{1}H NMR the signal at 3.65 ppm indicates methoxy group (A_{ME}) of FAME and signal at 2.28 ppm corresponding to methylene group (A_{CH2}). The presence of these signal in the biodiesel sample verifies the presence of methyl ester. Apart from the signal used for the quantification, there are other identifiable peaks such as signal at 0.86 to 0.87 ppm for CH_2-CH_3 or for latter methyl group. The peaks in the range of 1.24 to 2.34 represent CH_2 (methylene group). The signals at 5.3 range indicate presence of CH=CH (double bond) groups or olefinic groups[29-31]. In ^{13}C NMR the signal at 174.25 ppm and 51.35 indicates as peak for ester carbonyl –COO- and C-O respectively. The unsaturation in biodiesel sample was confirmed with help of signals at 131.88 ppm and 127.05 ppm. In addition to these signals, there are other signals at 14.03 ppm and 14.19ppm indicating the presence of terminal $–CH_3$ groups. The presence of $-CH_2$ group was showed with help of signals in the region of 22-34ppm[29]

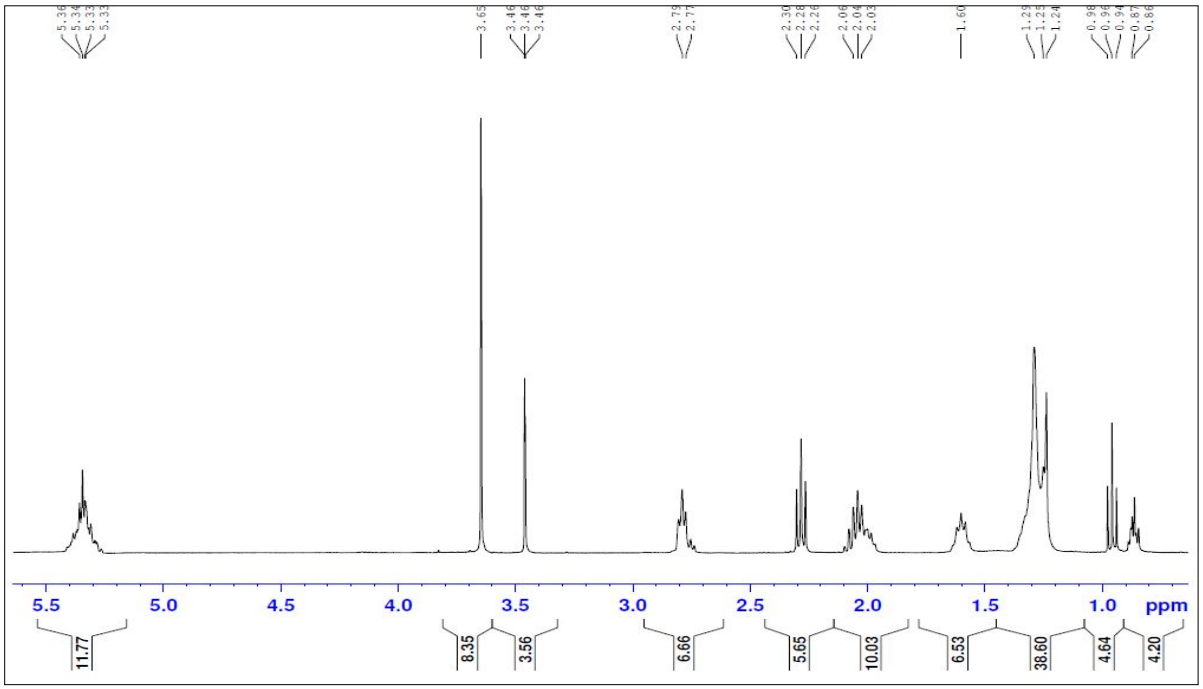

Figure 8 a. The ^{1}H NMR for the biodiesel sample obtained with TiO_2- $0.5C_4H_5KO_6$

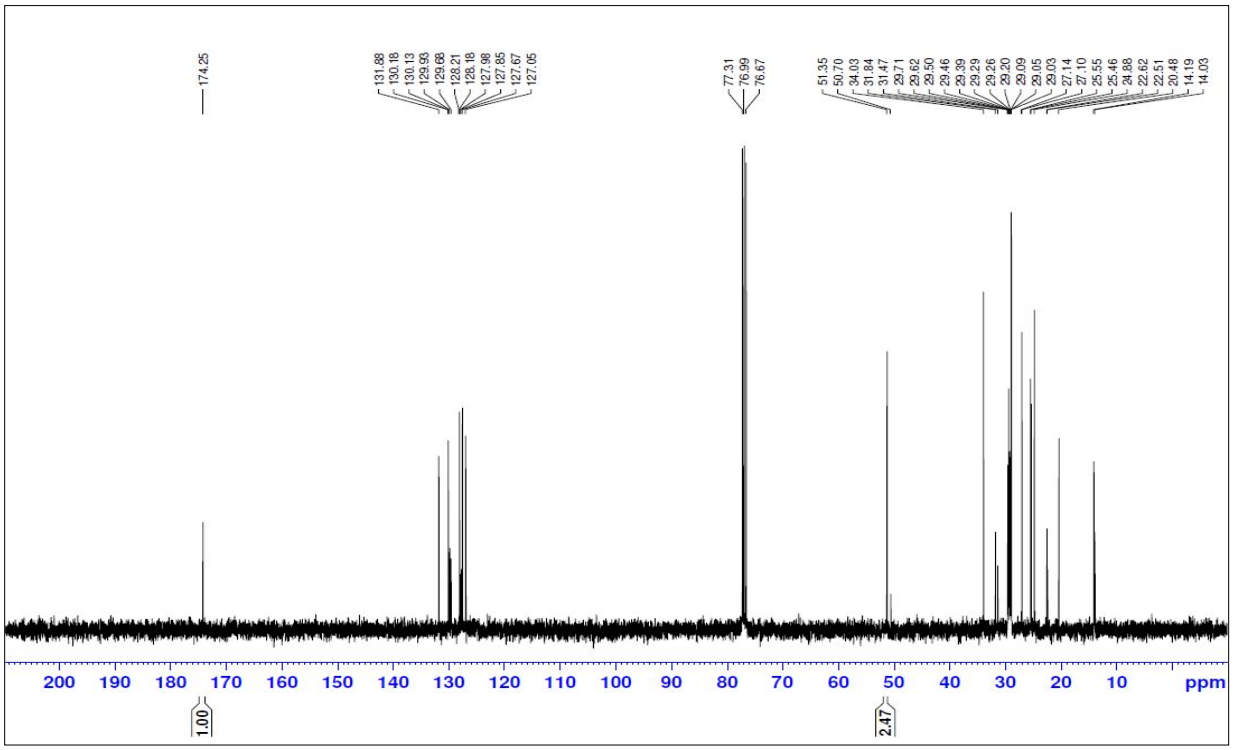

Figure 8 b. The ^{13}C NMR for the biodiesel sample obtained with TiO_2- $0.5C_4H_5KO_6$

3.4. Influence of various parameters on biodiesel production

The yield of biodiesel depends on the reaction conditions such as methanol to oil ratio, temperature, time, catalyst amount. Based on the preliminary screening of catalysts, TiO_2-$C_4H_5KO_6$ (1:0.5molar ratio) was found to be a more efficient catalyst for the conversion of linseed oil to fatty acid methyl ester. The optimum reaction conditions for higher conversion of linseed oil to biodiesel using TiO_2-$0.5C_4H_5KO_6$ was determined by a series of transesterification reactions.

3.4.1 Catalyst amount (weight %)

The influence of catalyst concentration on transesterification was studied by performing reactions at various catalyst concentration from 3 wt% to 12 wt% of the oil. The 98.5 % of biodiesel conversion was obtained within 3 h of reaction time at 60°C by using 6 wt% catalyst and 1:6 oil to methanol molar ratio (Figure 9a). The conversion of oil to biodiesel depends on catalyst amount, if the catalyst amount is lower than optimum concentration; there is reduction in FAME conversion due to decrease in the availability of active sites and hindrance to phase separation[19,25,32].

3.4.2 Oil to methanol molar ratio

Figure 9b depicts that the biodiesel conversion progressively rises from when oil to methanol molar ratio was increased from 1:3 to 1:6. The reaction was carried out at 6 wt% catalyst at 60°C for 3h of reaction time. The biodiesel conversion was negatively affected by increasing methanol concentration above the optimum value which was due to the increased solubility of glycerol to ester phase resulting in difficulty in separation of biodiesel. It may also favor the reverse reaction than the production of biodiesel[33,34].

3.4.3 Temperature

The effect of temperature on biodiesel yield was investigated by conducting the reaction at various temperatures using 6 wt% catalyst, 1:6 oil to methanol molar ratio for 3h reaction time (Figure 9c). The FAME conversion increased significantly up to 60°C and resulted in an optimum yield of fatty acid methyl esters. After 60°C biodiesel conversion decreased with increase in temperature, which is due to the fact that elevated temperature favors vaporization of methanol[25, 35,36].

3.4.4 Time

The influence of reaction time on transesterification reaction was examined by performing reactions for different time intervals using 6 wt% catalyst, 1:6 oil to methanol molar ratio at 60°C depicted in Figure 9d. The percentage of FAME conversion rose with the increase in reaction time up to 180 min and reached at its maximum. After 180 min instead of an increase in the yield of biodiesel, reduction in ester content with an increase in reaction time was observed. This is due to the reversible nature of transesterification reaction. After a prolonged reaction time backward reaction / reverse reaction of transesterification reaction is favored which leads to the hydrolysis of esters[35,37].

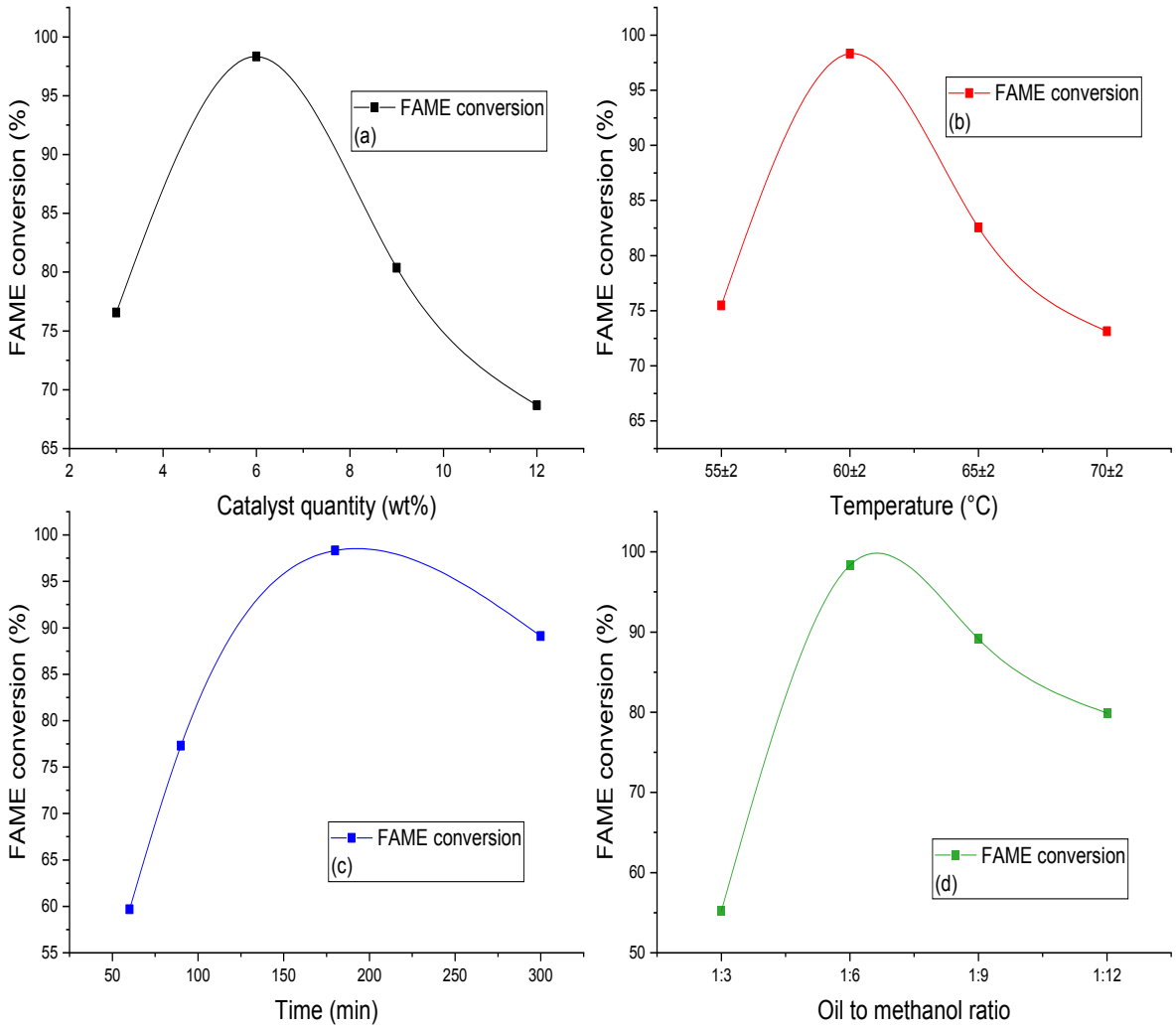

Figure 9. (a). Influence of catalyst amount (weight %) on biodiesel yield (b). Influence of oil to methanol molar ratio on biodiesel yield (c). Influence of reaction temperature on biodiesel yield (d). Influence of reaction time on biodiesel yield.

3.5. Properties of synthesized biodiesel from linseed oil

The properties of linseed oil methyl esters were determined using EN 14214/ ASTM D6751 method as shown in Table 5. All these parameters play an important role in biodiesel quality. The acid value of linseed oil methyl ester was found to be 0.3 mg KOH/g and it was within the limits of EN ISO method. The increase in acid value can create issues like corrosion of rubber parts of engine and filter clogging[38]. The other two important fuel parameters which influence the fuel injection operation are density and kinematic viscosity. Higher values of this can adversely affect the fuel injection process and result in the formation of engine deposits[39,40]. The density and kinematic viscosity of linseed oil methyl esters were 891.52 kg/m^3 and 3.5709 mm^2/s respectively. The other parameter is the flash point which indicates the minimum temperature at which fuel starts to ignite. It is important to know flash point value for fuel handling and storage [41]. The rest of the preferred features such as calorific value, cloud point, cetane number, and pour point are also within EN ISO/ASTM limits.

Table 5.

Properties of linseed oil methyl esters (TiO_2-0.5 $C_4H_5KO_6$ catalyst at concentration of 6wt%, 1:6 oil to methanol ratio, reaction temperature 60°C, reaction time 3h)

Property	EN 14214 test method	Limits	Methyl ester from linseed oil
Acid value (mg KOH/g)	Pr EN14104	0.5 max	0.3
Density at 15°C (kg/m^3)	EN ISO 12185	860-900	891.52
Kinematic viscosity at 40°C mm^2/s	EN ISO 3104	3-5	3.5709
Flash point (°C)	EN ISO 2719	-	173°C
Cetane Number	EN ISO 5165	≥51	57
Cloud point (°C)	D2500		4
Pour point (°C)	ISO 3016		2
Calorific value (MJ/kg)	D6751		40.89

3.6. Reusability and stability of catalyst

The catalyst reusability concept makes transesterification process cost effective and eco-friendlier. The catalyst deactivation is mainly due to deposition of impurities, oil content or thermal deactivation. The regeneration of catalyst usually attained with help of suitable solvent washing and calcination[42]. To analyze the reusability of TiO_2-0.5 $C_4H_5KO_6$ nanocatalyst, firstly it was separated from linseed oil methyl esters and glycerol. After

transesterification, the separated catalyst was washed several times with heptane to remove impurities. The washed catalyst was dried at 90°C and calcined at 500°C for 3h to reactivate the catalyst. The catalytic reusability of TiO_2-0.5 $C_4H_5KO_6$ over linseed oil using 6 wt% catalyst, 1:6 oil to methanol molar ratio within 180 min of reaction time at 60°C represented in Figure 10. Linseed oil to FAME conversion was decreased from 98.5% to 93.1%, respectively, in five cycles.

Stability of nanocatalyst after different cycles were evaluated by determining the leached metal ion concentration depicted in Figure 10. Inductively coupled plasma (ICP, Agilent 5110) was used to measure metal concentration. It was detected that from cycle 1 to cycle 5, the Li concentrations in solution are less than 0.043 mg/L. Moreover, Ti concentration in solution was null up to three cycles after that there was a slight leaching of Ti ions to solution which is less than 0.0004 mg/L

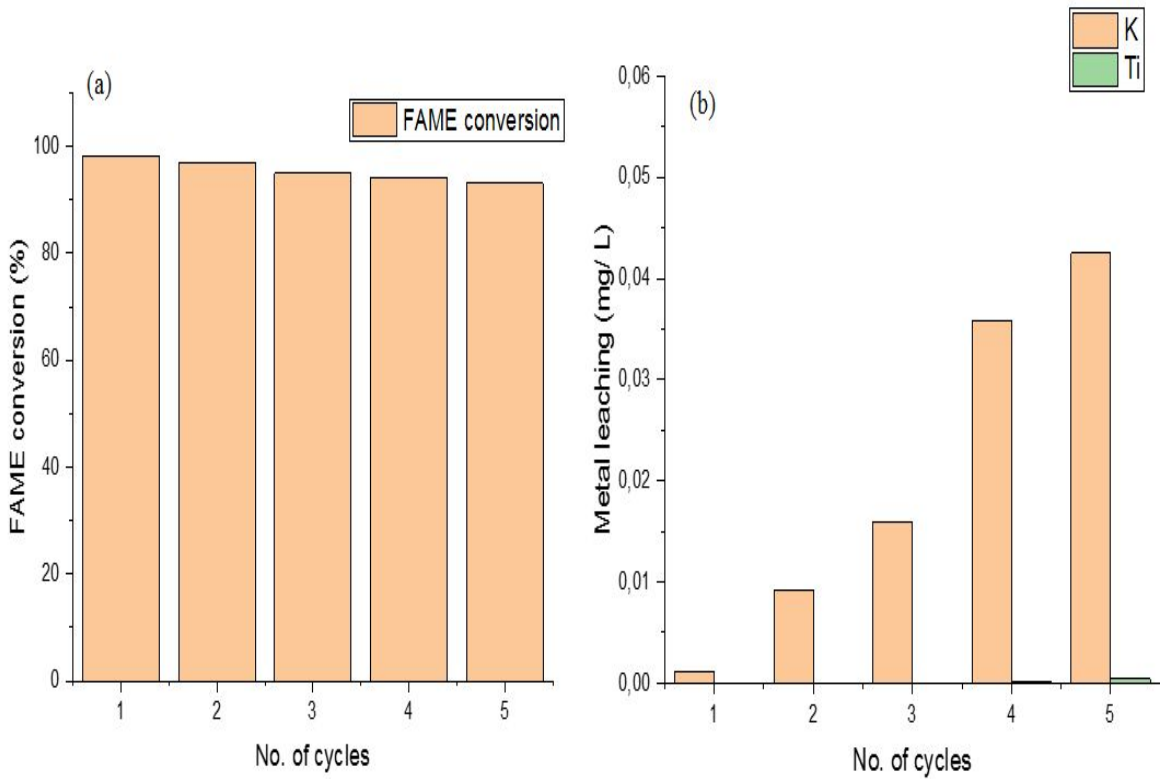

Figure 10. Reusability analysis of TiO_2-0.5 $C_4H_5KO_6$ catalyst up to five transesterification reactions

4. Conclusion

The biodiesel was successfully synthesized from linseed oil with help of TiO_2-0.5 $C_4H_5KO_6$. The modification of TiO_2 with $C_4H_5KO_6$ enhanced the properties of nanocatalyst due to impregnation of potassium and showed better conversion in comparison to unmodified TiO_2. FTIR, XRD, SEM, TEM, AFM confirmed the integration of potassium ions to TiO_2 nanostructure. The best activity was obtained at an optimum loading of $C_4H_5KO_6$ to TiO_2 in 0.5:1 molar ratio. The nanocatalyst showed 98.5 % fatty acid methyl ester content using 6wt % catalyst amount, 1:6 methanol ratio at 60°C within a reaction time of 3h. The properties of biodiesel such as acid value, density, kinematic viscosity and flash point were within the EN 14214 limits. Thus, FAME obtained was of good quality. All these results supports the efficient performance of TiO_2-0.5 $C_4H_5KO_6$ as a catalyst for the biodiesel production from linseed oil as a feedstock. The reusability of the catalyst also showed a promising result, which makes it economically feasible.

References

[1] Demirbas A. Importance of biodiesel as transportation fuel. *Energy Policy* 2007, 35, 4661-4670.

[2] Singh SP, Singh D. Biodiesel production through the use of different sources and characterization of oils and their esters as the substitute of diesel: A review. *Renew Sustain Energy Rev* **2010**, 14, 200–216. doi:10.1016/j.rser.2009.07.017.

[3] Li Y, Qiu F, Yang D, Li X, Sun P. Preparation, characterization and application of heterogeneous solid base catalyst for biodiesel production from soybean oil. *Biomass and Bioenergy* **2011**,35, 2787–2795.

[4] Rashtizadeh E, Farzaneh F. Transesterification of soybean oil catalyzed by Sr-Ti mixed oxides nanocomposite. *J Taiwan Inst Chem Eng* **2013**, 44, 917–923.

[5] Hu S, Guan Y, Wang Y, Han H. Nano-magnetic catalyst KF/CaO-Fe_3O_4 for biodiesel production. *Appl Energy* **2011**, 88, 2685–2690.

[6] Liu H, Su L, Shao Y, Zou L. Biodiesel production catalyzed by cinder supported CaO/KF particle catalyst. *Fuel* **2012**, 97, 651–657.

[7] Madhuvilakku R, Piraman S. Biodiesel synthesis by TiO_2-ZnO mixed oxide nanocatalyst catalyzed palm oil transesterification process. *Bioresour Technol* **2013**, 150, 55–59.

[8] Qiu F, Li Y, Yang D, Li X, Sun P. Heterogeneous solid base nanocatalyst: Preparation, characterization and application in biodiesel production. *Bioresour Technol* **2011**, 102,

4150–4156.

[9] Kaur M, Ali A. Lithium ion impregnated calcium oxide as nano catalyst for the biodiesel production from karanja and jatropha oils. *Renew Energy* **2011**, 36, 2866–2871.

[10] Baskar G, Selvakumari IAE, Aiswarya R. Biodiesel production from castor oil using heterogeneous Ni doped ZnO nanocatalyst. *Bioresour Technol* **2018**, 250, 793–798.

[11] Ding H, Ye W, Wang Y, Wang X, Li L, Liu D, et al. Process intensification of transesterification for biodiesel production from palm oil : Microwave irradiation on transesterification reaction catalyzed by acidic imidazolium ionic liquids *Energy* **2018**, 144, 957-967.

[12] Teo SH, Islam A, Taufiq-Yap YH. Algae derived biodiesel using nanocatalytic transesterification process. *Chemical engineering research and design* **2016**, 111, 362–370.

[13] Ambat I, Srivastava V, Sillanpää M. Recent advancement in biodiesel production methodologies using various feedstock : A review . *Renewable and sustainable energy reviews* **2018**, 90, 356–369.

[14] Aransiola EF, Ojumu T V., Oyekola OO, Madzimbamuto TF, Ikhu-Omoregbe DIO. A review of current technology for biodiesel production: State of the art. *Biomass and Bioenergy* **2014**, 61, 276–297.

[15] Kumar R, Tiwari P, Garg S. Alkali transesterification of linseed oil for biodiesel production. *Fuel* **2013**, 104, 553–560.

[16] Gargari MH, Sadrameli SM. Investigating continuous biodiesel production from linseed oil in the presence of a Co-solvent and a heterogeneous based catalyst in a packed bed reactor. *Energy* **2018**, 148, 888–895.

[17] Akia M, Yazdani F, Motaee E, Han D, Arandiyan H. A review on conversion of biomass to biofuel by nanocatalysts. *Biofuel Res J* **2014**,1, 16–25.

[18] Hashmi S, Gohar S, Mahmood T, Nawaz U, Farooqi H. Biodiesel Production by using CaO-Al_2O_3 Nano Catalyst. *Int J Eng Res Sci* **2016**, 2, 2395–6992.

[19] Takase M, Chen Y, Liu H, Zhao T, Yang L, Wu X. Biodiesel production from non-edible Silybum marianum oil using heterogeneous solid base catalyst under ultrasonication. *Ultrason Sonochem* **2014**, 21, 1752–62.

[20] Fadhil AB, Al-tikrity ETB, Khalaf AM. Transesterification of non-edible oils over potassium acetate impregnated CaO solid base catalyst. *Fuel* **2018**, 234, 81–93.

[21] Fadhil AB, Aziz AM, Altamer MH. Optimization of methyl esters production from non-edible oils using activated carbon supported potassium hydroxide as a solid base catalyst. *Arab J Basic Appl Sci* **2018**, 25, 56–65.

[22] Buasri A, Worawanitchaphong P, Trongyong S. Utilization of Scallop Waste Shell for Biodiesel Production from Palm Oil - Optimization Using Taguchi Method. *Procedia - Soc Behav Sci* **2014**, 8, 216–221.

[23] Bagheri S, Julkapli NM, Bee S, Hamid A. Titanium Dioxide as a Catalyst Support in Heterogeneous Catalysis . *The scientific world journal* **2014**, doi.org/10.1155/2014/727496.

[24] Thitsartarn W, Kawi S. An active and stable CaO – CeO 2 catalyst for transesterification of oil to biodiesel. *Green Chemistry* **2011**, 13, 3423- 3430.

[25] Singh V, Bux F, Sharma YC. A low cost one pot synthesis of biodiesel from waste frying oil (WFO) using a novel material, β-potassium dizirconate (β-$K_2Zr_2O_5$). *Appl Energy* **2016**, 172, 23-33.

[26] Yan S, Kim M, Salley SO, Ng KYS. Oil transesterification over calcium oxides modified with lanthanum. *Applied Catalysis A : General* **2009**, 360, 163–170.

[27] Wang X, Xiang Q, Liu B, Wang L, Luo T, Chen D, et al. TiO_2 modified FeS Nanostructures with Enhanced Electrochemical Performance for Lithium-Ion Batteries . *Scientific reports*: **2013, 3,** 1–8.

[28] Hu S, Li F, Fan Z, Wang F, Zhao Y, Lv Z. Band gap-tunable potassium doped graphitic carbon nitride with enhanced mineralization ability. *Dalton Trans.* **2015**,44, 1084-1092.

[29] Tariq M, Ali S, Ahmad F, Ahmad M, Zafar M, Khalid N, et al. Identification, FT-IR, NMR (1H and 13C) and GC/MS studies of fatty acid methyl esters in biodiesel from rocket seed oil. *Fuel Process Technol* **2011**, 92, 336–341.

[30] Thangaraj B, Piraman S. Heteropoly acid coated ZnO nanocatalyst for Madhuca indica biodiesel synthesis. *Biofuels* **2016**, 7(1), 13–20.

[31] Mello VM, Oliveira FCC, Fraga WG, Claudia J, Suarez PAZ. Determination of the content of fatty acid methyl esters (FAME) in biodiesel samples obtained by esterification using 1 H-NMR spectroscopy. *MagnResonChem* **2008**, 46, 1051–1054.

[32] Encinar JM, Pardal A, Sánchez N. An improvement to the transesterification process by the use of co-solvents to produce biodiesel. *Fuel* **2016**, 166, 51–58.

[33] Banihani FF. Transesterification and Production of Biodiesel from Waste Cooking Oil : Effect of Operation Variables on Fuel Properties. *American Journal of Chemical Engineering* **2017**, 4, 154–160.

[34] Kafui G, Sunnu A, Parbey J. Effect of biodiesel production parameters on viscosity and yield of methyl esters : Jatropha curcas , Elaeis guineensis and Cocos nucifera. *Alexandria Eng J* **2015**, 54,1285–1290.

[35] Eevera T, Rajendran K, Saradha S. Biodiesel production process optimization and characterization to assess the suitability of the product for varied environmental conditions. *Renew Energy* **2009**, 34, 762–765.

[36] Abbah EC, Nwandikom GI, Egwuonwu CC, Nwakuba NR. Effect of Reaction Temperature on the Yield of Biodiesel From Neem Seed Oil. *Am J Energy Sci* **2016**, 3, 16–20.

[37] Ofoefule AU, Ibeto CN, Ugwu LC, Eze DC. Determination of Optimum Reaction Temperature and Reaction Time for Biodiesel Yield from Coconut (Cocos nucifera) Oil. *International Research Journal of Pure & Applied Chemistry **2014***, 4(1), 108-117

[38] Chhetri AB, Watts KC, Islam MR. Waste Cooking Oil as an Alternate Feedstock for Biodiesel Production. *Energies* **2008**,1, 3–18.

[39] Demirbas A. Biodiesel: A realistic fuel alternative for diesel engines. Biodiesel A Realis Fuel Altern Diesel Engines 2008:1–208. doi:10.1007/978-1-84628-995-8.

[40] Knothe G, Steidley KR. Kinematic viscosity of biodiesel fuel components and related compounds. Influence of compound structure and comparison to petrodiesel fuel components. *Fuel* **2005**, 84, 1059–1065.

[41] Aleme HG, Barbeira PJS. Determination of flash point and cetane index in diesel using distillation curves and multivariate calibration. *Fuel* **2012**, 102, 129–134.

[42] Prescott W V., Schwartz AI. Nanorods and Nanomaterials Research Progress **2008**, Nova science publishers, ISBN 978-1-60456-122-7 .